

Recombination coefficient analysis of hydrogen plasma species in the afterglow regime

Felix Boy Martupa Sihombing^{1*}, Saktioto¹, Kusherbayeva Maikul²,
Kushkimbayeva Bibara²

¹Department of Physics, Universitas Riau, Pekanbaru 28293, Indonesia

²Department of Physics and Informatics, M. Kh. Dulati Taraz State University, Taraz 12984, Kazakhstan

ABSTRACT

The recombination coefficient of hydrogen plasma using the six thermal hydrogen species in the afterglow condition was analyzed through MATLAB computational modeling to determine the logarithmic density, and then to determine the difference between conduction and convection. This study aims to model the dynamics of recombination and determine the recombination coefficients of hydrogen species against temperature variations. This modeling was carried out using zero-dimensional chemical kinetic equations derived from the continuity equation, namely the reaction rate calculated using modified Arrhenius. This modeling is integrated numerically using the Runge-Kutta method. The density results of hydrogen species show a consistent decrease in temperature variation related to the ideal gas law, but the recombination coefficient increases with increasing temperature. This upward trend indicates that there is a dominance of three-body recombination processes over atmospheric pressure and afterglow conditions.

ARTICLE INFO

Article history:

Received Nov 26, 2025

Revised Feb 23, 2026

Accepted Feb 25, 2026

Keywords:

Chemical Kinetics
Plasma Diffusion
Runge-Kutta Integration
Thermal Equilibrium
Three-Body Process

This is an open access article under the [CC BY](#) license.



Corresponding Author

E-mail address: felix.boy4495@student.unri.ac.id

1. INTRODUCTION

Atmospheric pressure plasma is generated when electrical energy is converted into energetic electrons that collide with neutral gas species. These collisions follow probabilistic mechanisms consisting of elastic collisions, which do not alter the internal energy of neutral species, and inelastic collisions, which modify the electronic structure of atoms and molecules, potentially creating excited species when sufficient energy is transferred [1]. Excited species generally possess short lifetimes and return to the ground state through photon emission, while metastable species exhibit longer lifetimes due to inhibited radiative transitions.

Thermal plasma under local thermodynamic equilibrium (LTE) is characterized by equal electron and heavy particle temperatures ($T_e = T_h$), high electron densities ranging from 10^{21} to 10^{26} m^{-3} , and dominant collisional processes rather than radiative transitions [2]. In such systems, micro-reversibility must be satisfied, meaning excitation is balanced by de-excitation and ionization by recombination. The formation and maintenance of plasma jets at atmospheric pressure are governed by breakdown conditions described by Paschen's law, which relates discharge voltage to gas pressure and electrode distance [3]. At sufficiently high pressures, frequent electron-gas collisions enable energy transfer that leads to thermal plasma conditions with temperatures on the order of $10^3 - 10^4 \text{ K}$ [4].

From the perspective of chemical kinetic theory, plasma behavior can be described using the ideal gas relation $p = nk_B T$, where pressure is proportional to particle density and temperature [5]. Plasma thermodynamic equilibrium is achieved when density, temperature, mass, and pressure remain balanced before and after collisions. This equilibrium can be classified into macroscopic and microscopic equilibrium states.

A key process governing plasma decay is recombination, defined as the interaction between electrons and ions to form neutral atoms, often accompanied by photon emission [6]. Two primary recombination mechanisms are recognized: three-body recombination, involving two electrons and one ion [7], and radiative recombination, in which a free electron is captured while emitting photon energy [8]. During the afterglow phase, plasma transitions into neutral gas as temperature gradually decreases, often producing observable luminescence phenomena such as chemiluminescence or phosphorescence [9].

The recombination coefficient represents the effectiveness of recombination processes and depends on plasma parameters such as density, temperature, and pressure. Surface-related recombination mechanisms include the Eley–Rideal and Langmuir–Hinshelwood models [10]. For computational simplicity, zero-dimensional (0D) global models are frequently employed under the assumption of spatially uniform radical density and simplified flux boundary conditions [11-13]. Such modeling approaches enable the determination of radical densities and recombination coefficients under varying plasma conditions, particularly in atmospheric-pressure afterglow systems.

2. LITERATURE REVIEW

2.1. Atmosphere Pressure Plasma

The atmospheric pressure plasma is referred to as the result of electrical energy converting the electric field into gas electrons, which are then carried to neutral species in the form of collisions. Collisions follow probabilistic laws, including: (1) elastic collisions that do not change the internal energy of neutral species, and (2) inelastic collisions that change the electronic structure of neutral species, creating excited species if the energy to perform the collision is sufficient [1].

Each excited species has a short lifetime and is in a ground state by emitting photon energy. “Metastable species” include excited states, but with long lifetimes because decay by radiation emission is inhibited due to the absence of possible transitions from each state: decay only occurs when energy is transferred through collision.

Table 1. Main characteristics of LTE plasma.

Characteristics	LTE plasma
Current name	Thermal plasma
Properties	<ul style="list-style-type: none"> • $T_c = T_h$ • High electron density: $10^{21} - 10^{26} \text{ m}^{-3}$ • Inelastic collisions between electrons and heavy particles create reactive plasma species, while elastic plasma heats heavy particles.
Example	Plasma arc (core) $T_c = T_h$ $\approx \approx$ 10,000 K

Table 1 shows the properties of LTE plasma, currently referred to as thermal plasma. Thermal plasma has the same cold temperature properties as hot temperatures. The electron density in thermal plasma is between 10^{21} and 10^{26} m^{-3} , which is a high electron density. Thermal plasma involves inelastic collisions between electrons and heavy particles, resulting in reactive species in the plasma. Meanwhile, elastic collisions can heat heavy particles.

LTE plasma requires transitions and chemical reactions governed by collisions rather than by radiative processes. In addition, collision phenomena must be microreversible. This means that each type of collision must be balanced by its opposite (excitation/de-excitation; ionization/recombination; kinetic equilibrium) [2].

Plasma jet discharge can be ignited and plasma can be maintained if the DC voltage applied to the gas medium is higher than the breakdown voltage and product if the DC voltage is applied through the electrodes – where p is the gas pressure and d is the distance between the electrodes referred to as Paschen's law [3].

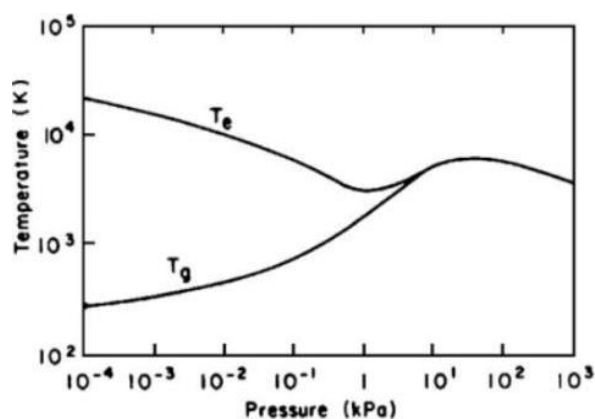


Figure 1. Evolution of electron temperature and heavy particle plasma with pressure in plasma.

Figure 1 shows a graph of pressure versus temperature, illustrating the effect of pressure on the transition from light emission ($T_c > T_h$) to arc emission. At high pressures, electrons and gas collide with each other until the electrons transfer energy to the gas. Thus, when the temperature is at a pressure of 10 kPa, a thermal plasma occurs in a state of equilibrium with temperatures of 10^3 and 10^4 K [4].

1.2. Chemical Kinetic Theory

The kinetic theory of gases describes gases as a large collection of small particles that move randomly and constantly. These gas atoms collide with each other and with the walls of the container. This explains the macroscopic properties of gases, such as pressure, temperature, and volume.

The general equation for ideal gases in statistical mechanics is generally formulated as [5]:

$$p = nk_B T \quad (1)$$

where p is pressure, n is number density, k_B is the Boltzmann constant equal to 1.3807×10^{-23} J/K, and T is temperature. According to the Compendium of Chemical Terminology, published by IUPAC in 1997, number density is the number of particles per unit volume, with the unit m^{-3} . In plasma, there are two types of charged particles, namely light electrons and heavy ions.

Thermodynamic equilibrium of plasma will be achieved when the particle density, temperature, mass, and pressure of the plasma system before and after collision are the same. When the density of plasma species before and after collision is the same, it is called density equilibrium. Thermodynamic equilibrium of plasma consists of two types: macroscopic and microscopic equilibrium.

1.3. Recombination Process

Recombination is the process of combining electrons and ions to form neutral atoms in the form of gas. This recombination process was first studied by researching atoms and ions from hydrogen species. Recombination also occurs when electrons and ions collide to form neutral atoms with the emission of photon energy [6]. There are two methods of plasma recombination: (1) three-body recombination, where ions, electrons, and neutral atoms are in the same process, with the recombination of three objects which involves two electrons and an ion forming a neutral atom through the formation of ion molecules and molecules [7]. Meanwhile, (2) radiative recombination refers to the capture of free electrons in releasing one or more photon energies [8].

Recombination that converts plasma into neutral gas will cause decay, whereby the gas temperature gradually cools down following the cessation of high-energy release, known as the afterglow condition. When gas undergoes decay, plasma often emits light, which is found, for example, in the chemiluminescence or phosphorescence of certain chemical elements [9].

Next, the recombination coefficient is defined as the ratio of atoms that are prominent on the surface and react to form molecules to the total number of atoms that are prominent on the surface, which is referred to as the Haftungskoeffizient defined by Paneth and Herzfeld. Currently, two

recombination mechanisms are considered, namely Eley-Rideal (ER) and Langmuir-Hinshelwood (LT). ER states that the absorption reaction of atoms on the surface occurs directly with atoms from the gas phase. Meanwhile, LT states that recombination only occurs on the adatom surface [10].

The simple zero-dimensional model is used to determine the radical density measurements of each gas. The model is simulated by four different powers for all pressure points. There are necessary assumptions regarding the zero-dimensional model. First, the radical density is uniform in a given space [11]. Second, the charge density is assumed to be parabolic [12]. Furthermore, constructing a model that predicts density on the surface wall would increase the complexity even further; Thus, a simple spatial geometry is used to calculate the flux boundary [13], so that the model considers a small box as the geometric domain in the space between the radical probe and Langmuir. In a small domain, the plasma is considered uniform and the net flux across the box surface is set to zero, so that there is no net flux across the surface and the nonaxial dimensions are variable. However, the size of the domain can be calculated using the area-to-volume ratio A/V .

3. RESEARCH METHODS

This study uses quantitative research conducted computationally using MATLAB software with the Runge-Kutta method. The Runge-Kutta method is used to solve the continuity of ordinary differential equation systems mathematically using numerical integrators to handle nonlinear, coupled, and time-dependent systems. The MATLAB solver ode45 was used to handle stiff computational problems.

The continuity equation describes the chemical kinetic model applied to each chemical species, including hydrogen. The continuity equation can be formulated from Ismail et al. (2011) [14]:

$$\frac{\partial n}{\partial t} + \nabla(nv) = S \quad (1)$$

where, n is the density, v is the velocity depending on position, and S is the production rate of the species per unit volume (m^3/s).

The reaction of a species can be shown by the following equation [15]:



meanwhile, the forward reaction rate is given by:

$$R_f = k_f(n_A)^a(n_B)^b \quad (3)$$

and the reverse reaction rate is given by:

$$R_r = k_r(n_C)^c(n_D)^d \quad (4)$$

where, A , B , C , and D are the species involved in the reaction, and n indicates the density of the species. Meanwhile, a , b , c , and d are the coefficients of each particle in a reaction.

The Arrhenius equation has only a temperature function. The higher the temperature, the faster the collision speed. Meanwhile, the lower the temperature, the slower the collision speed. The factor that causes the speed of collisions in each reaction depends on the values of the parameters α , β , and γ shown in the modified Arrhenius equation.

The modified Arrhenius equation is defined as an explanation of the dependence of the pre-exponential factor on temperature. The modified Arrhenius equation can be written in the form:

$$k = \alpha T^\beta e^{-\frac{\gamma}{T}} \quad (5)$$

where, α is the value of the ability of the number of particles colliding per second. The value of β is the effect of the function of the number of particles colliding. Meanwhile, the value of γ is the effect of the activation energy of each particle collision.

4. RESULTS AND DISCUSSION

4.1. Density Variation of Hydrogen Plasma Species

Computational modeling using MATLAB with the ode45 solver then determines the density and logarithmic density results for the species e^- , H, H^+ , H_2^+ , H_3^+ , and H_2 with temperature variations ranging from 0.001 eV (equivalent to 11.6 K) to 0.009 eV; 0.01 eV (equivalent to 116 K) to 0.09 eV; and 0.1 eV (equivalent to 1,160 K) to 0.9 eV. Each of these temperature groups has different density and logarithmic density values for each hydrogen species as the temperature of the released plasma jet increases.

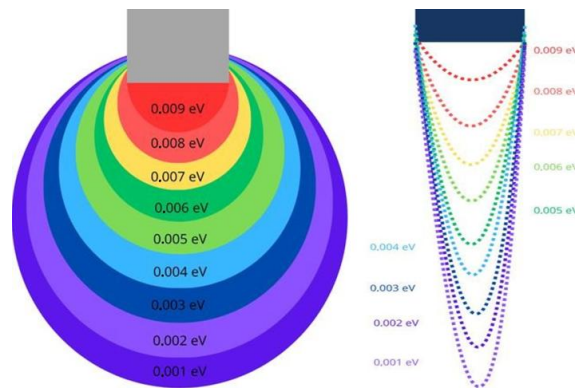


Figure 2. (a) Launch of a hydrogen plasma jet with recombination radiation distances between temperatures of 0.001 and 0.009 eV, and (b) End of the process when the plasma cools and the radiation level decreases.

Figure 2 shows the launch of a plasma jet until it releases radiation from hydrogen plasma. After the launched plasma undergoes recombination, the radiation from the plasma gradually cools with increasing distance from the plasma jet source. However, despite the cooling temperature between 0.001 and 0.009 eV that is recombined, the density of each hydrogen species has a very large density value which then decreases slowly with increasing temperature.

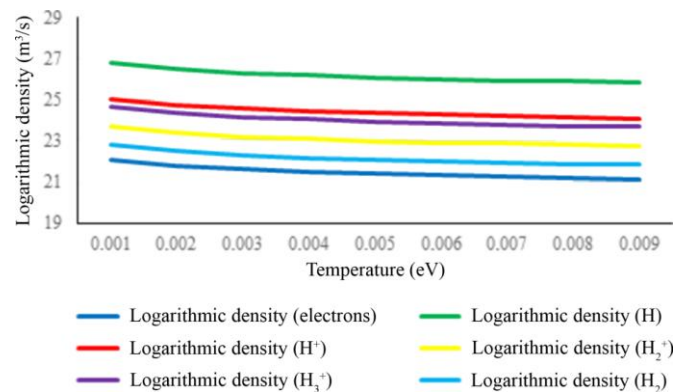


Figure 3. Hydrogen logarithmic density at temperatures ranging from 0.001 to 0.009 eV.

Figure 3 shows a decrease in logarithmic density at temperatures of 0.001 to 0.009 eV, with the highest logarithmic density values found in atomic species H, ranging from 26.7885 to 25.9342, while the lowest values are found in electron ion species, ranging from 22.0895 to 21.1353. This is related to the ideal gas law, where a decrease in total density must be balanced by an increase in temperature at high pressure, including atmospheric pressure. Figure 3 also shows a decrease in density that appears to flatten out near zero. This is related to the integration of density over time to ensure that the density integration is in equilibrium, or reaches a state of thermodynamic equilibrium.

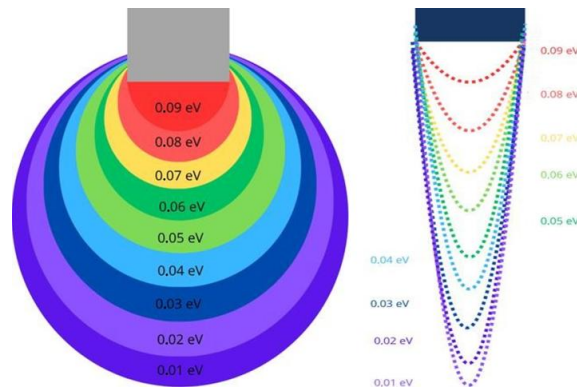


Figure 4. (a) Launch of a hydrogen plasma jet with recombination radiation distances between temperatures of 0.01 and 0.09 eV, and (b) End of the process when the plasma cools and the radiation level decreases.

Figure 4 shows the launch of a plasma jet until it releases radiation from hydrogen plasma. After the launched plasma undergoes recombination, the radiation from the plasma gradually cools down with increasing distance from the plasma jet source. However, despite the cooling temperature between 0.01 and 0.09 eV that is recombined, the density of each hydrogen species decreases due to the increasing temperature, which widens the distance between ions and atoms, thereby reducing the density of each species.

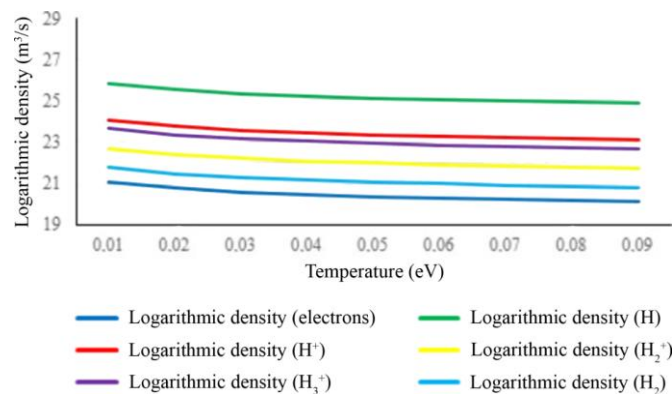


Figure 5. Hydrogen logarithmic density at temperatures ranging from 0.01 to 0.09 eV.

Figure 5 above shows the results of the logarithmic density of hydrogen plasma species between 0.01 and 0.09 eV, which experiences a decrease in density as the temperature increases for each species. Figure 5 shows that plasma density at higher temperatures will decrease rapidly.

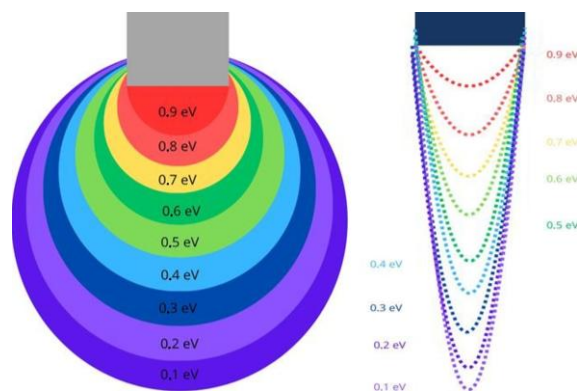


Figure 6. (a) Hydrogen plasma jet launch with radiation–recombination distances between 0.1 and 0.9 eV, and (b) End of the process when the plasma cools and the radiation level decreases.

Figure 6 shows a plasma jet emitting plasma that cools to 0.1 – 0.9 eV. At this temperature range, recombination occurs after the plasma becomes gas, affecting the density of hydrogen species and causing it to decrease rapidly. This density decrease affects the recombination coefficient, leading to faster decay. The logarithmic density for temperatures of 0.1 – 0.9 eV is shown in Figure 7.

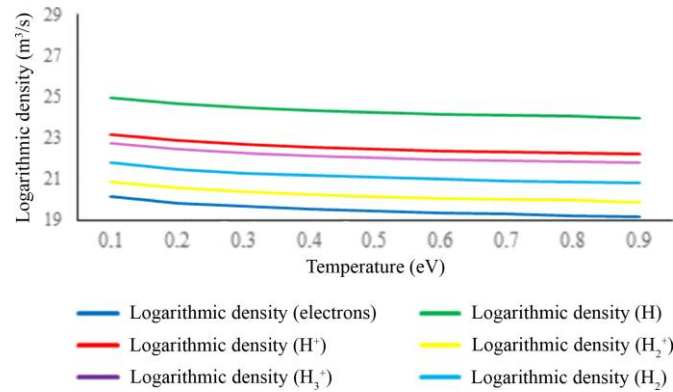


Figure 7. Logarithmic density at temperatures of 0.1 to 0.9 eV.

From the Figure 7 showing the density and logarithmic density of each hydrogen species at thermodynamic equilibrium, there is a decrease in density, where as the temperature increases, the density and logarithmic density decrease. The decrease in hydrogen species density is related to the ideal gas law (Saha equation). At constant pressure, increasing temperature reduces total density.

Recombination in the afterglow state must have low densities of electrons and hydrogen ions (e^- , H^+ , H_2^+ , H_3^+), while neutral atoms must have high densities (H and H_2). Meanwhile, the total density of heavy particles for ions and neutral atoms remains at a constant point in a closed system. However, the density of each hydrogen species has a higher density value than the initial electron density of 10^{15} m^{-3} , so this can be included in the recombination reaction process in the afterglow state.

3.2. Determination for the Recombination Coefficients of Hydrogen

To calculate the recombination coefficients of hydrogen species as the temperature increases (in eV), the following recombination coefficient equation is used:

$$\gamma = \frac{8}{nv_{th}W_{DA}} \left[\frac{S_x \chi}{L} (T_{cold} - T_{hot}) - h_c S (T_{hot} - T_{cold}) \right] \quad (6)$$

where γ is the recombination coefficient of hydrogen species with respect to temperature variation, expressed in volumetric form (m^3/s). Meanwhile, R_{rec} combines S_x , χ , and L (conductor parameters), h_c and S (convection parameters), and T_{hot} and T_{cold} , the temperatures measured near the probe.

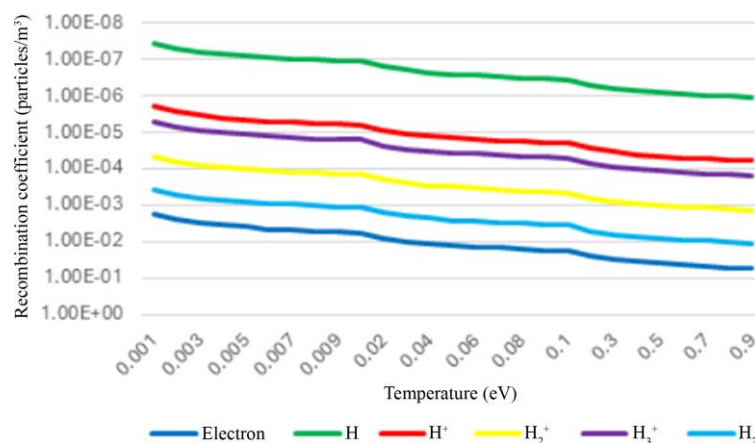


Figure 8. Graph of hydrogen recombination coefficients between 0.001 and 0.9 eV.

Figure 8 shows different recombination coefficients obtained through radical density with changes in plasma temperature. This indicates that large temperature changes increase the recombination coefficient of hydrogen species, depending on the radical density.

The increase in the recombination coefficient of each species is an effective coefficient that depends on plasma conditions. Generally, recombination processes, such as radiative recombination, decrease with increasing temperature, making hot electrons more difficult to capture. However, at high pressures (including atmospheric pressure) and high density of hydrogen species, the dominant recombination mechanism is the three-body process, which is radiative collision recombination.

5. CONCLUSION

This study has investigated that the recombination model under afterglow conditions has been determined through the plasma diffusion process. Furthermore, this study has successfully determined the plasma recombination coefficient under afterglow conditions for atmospheric pressure. Among them, the hydrogen plasma density from a temperature of 0.001 to 0.9 eV shows that the hydrogen plasma density decreases as the temperature increases. Meanwhile, for the recombination coefficient obtained from the radical density of each species, it was noted that the hydrogen plasma recombination coefficient increases as the temperature of a species increases, where the recombination coefficient is predominantly at temperatures below 0.1 eV. If the recombination coefficient value of each species is higher, the plasma density will quickly decays due to the diffusion process. Thus, it will emit light induced by recombination that is brighter, but with a shorter duration.

ACKNOWLEDGMENTS

The authors gratefully acknowledge Universitas Riau and LPPM Universitas Riau for supporting this research. Appreciation is also extended to the Kemendikisaintek and M.Kh. Dulati Taraz State University, Kazakhstan, for their support.

REFERENCES

- [1] Braithwaite, N. S. J. (2000). Introduction to gas discharges. *Plasma Sources Sci. Technol.*, **9**(4).
- [2] Moisan, M., Barbeau, J., Crevier, M. C., Pelletier, J., Philip, N., & Saoudi, B. (2002). Plasma sterilization. Methods and mechanisms. *Pure and Applied Chemistry*, **74**(3), 349–358.
- [3] Lieberman, M. A. & Lichtenberg, A. J. (1994). Principles of plasma discharges and materials processing. *MRS Bulletin*, **30**(12), 899–901.
- [4] Boulos, M. (1994). Thermal plasmas: fundamentals and applications. *Plenum*, **1**, 163.
- [5] Krall, N. A., Trivelpiece, A. W., & Gross, R. A. (1973). Principles of plasma physics. *American Journal of Physics*, **41**(12), 1380–1381.
- [6] Goldston, R. J. (2020). *Introduction to plasma physics*. CRC Press.
- [7] Cretu, M. T., Mirahmadi, M., & Pérez-Ríos, J. (2022). Ion-atom-atom three-body recombination in cold hydrogen and deuterium plasmas. *Physical Review A*, **106**(2), 023316.
- [8] Fritzsche, S., Maiorova, A. V., & Wu, Z. (2023). Radiative recombination plasma rate coefficients for multiply charged ions. *Atoms*, **11**(3), 50.
- [9] Gudem, M., Yadav, A., & Vijayan, A. (2025). Mechanism of chemiluminescence in the air afterglow reaction. *The Journal of Physical Chemistry A*, **129**(23), 5062–5072.
- [10] Qerimi, D., Panici, G., & Ruzic, D. N. (2021). Determination of recombination coefficients for hydrogen, oxygen, and nitrogen gasses via in situ radical probe system. *J. Vac. Sci. Technol. A*.
- [11] Bogaerts, A., Eckert, M., & Neyts, E. (2011). Computer modelling of the plasma chemistry and plasma-based growth mechanisms for nanostructured materials. *J. Phys. D: Appl. Phys.*, **44**(17).
- [12] Kim, W., Do, H., & Cappelli, M. A. (2006). Plasma-discharge stabilization of jet diffusion flames. *IEEE Transactions on Plasma Science*, **34**(6), 2545–2551.
- [13] Despiau-Pujo, E., Brihoum, M., & Cunge, G. (2014). Pulsed Cl₂/Ar inductively coupled plasma processing: 0D model versus experiments. *J. Phys. D: Appl. Phys.*, **47**(45), 455201.
- [14] Ismail, F. D., Saktioto, T., & Ali, J. (2011). Thermodynamic equilibrium for nitrogen species discharge: Comparison with global model. *Optik*, **122**(5), 455–458.
- [15] Hugill, J. & Saktioto, T. (2001). A simplified chemical kinetic model for slightly ionized, atmospheric pressure nitrogen plasmas. *Plasma Sources Science and Technology*, **10**(1), 38–42.